

# We are IntechOpen, the world's leading publisher of Open Access books Built by scientists, for scientists

4,800

Open access books available

122,000

International authors and editors

135M

Downloads

Our authors are among the

154

Countries delivered to

TOP 1%

most cited scientists

12.2%

Contributors from top 500 universities



WEB OF SCIENCE™

Selection of our books indexed in the Book Citation Index  
in Web of Science™ Core Collection (BKCI)

Interested in publishing with us?  
Contact [book.department@intechopen.com](mailto:book.department@intechopen.com)

Numbers displayed above are based on latest data collected.  
For more information visit [www.intechopen.com](http://www.intechopen.com)



---

# Electrochemical Materials Design for Micro-Supercapacitors

---

Can Liu and Zhengjun Zhang

Additional information is available at the end of the chapter

<http://dx.doi.org/10.5772/64986>

---

## Abstract

Micro-supercapacitors (m-SC) arise from the demand of developing micro-power system for MEMS devices, attracting much research interest in recent years. As m-SC has to achieve high areal energy and power densities, the volumetric capacitance and the rate capability of the electrode materials have become the most important concern. This review compares the intrinsic electrochemical properties of the state-of-art electrode materials for m-SC, reporting the recent advances in the three types of electrode materials. For carbon electrode materials, two developing trends are identified: one is to enhance volumetric capacitance through a proper film fabrication process, while the other one is to further promote its fast response rate by making open-structured devices. For pseudocapacitive oxides, in order to achieve better rate capability and cyclability, the relationship between the electrochemical property and the structure is worth further exploration. As an example, the composition, microstructure, and morphology of the molybdenum oxide film were optimized to realize superior electrochemical performance as an electrode material for m-SC. Architecture design is another important factor for m-SC. In-plane interdigital architectures have proven its success to fabricate fast response devices. Further study on the interplay effect between such architecture and pseudocapacitive materials is in need.

**Keywords:** micro-supercapacitors, electrode materials, EDLC, pseudocapacitance

---

## 1. Introduction

Since the microelectromechanical systems (MEMS) develop rapidly toward standalone microsensors, actuators, and various functional devices, the design of power supply has received more and more research interests [1]. The conventional bulky batteries severely limit

---

the advantages of these smart systems, a micropower system, i.e., generating power directly from microstructures, thus has to be developed [2]. After the earliest explorations on the micro-internal-combustion engine which requires complicated micromachining processes and high manufacturing cost [2–4], researchers turn to microbattery system which is potentially of low cost and high capacity and more desirable for MEMS devices [1]. A complete micropower system should consist of energy conversion and storage units integrated on chip. The energy conversion devices include microscaled fuel cells and solar cells, while the energy storage devices mainly refer to rechargeable microbatteries, which have been remarkably advanced under many research efforts [5]. Microbatteries, or thin-film batteries, have become commercially available with a rapid expanding market. Nevertheless, similar to the features of macro-scaled batteries, the shortages of microbatteries are limited lifetime and low power density, which bring economic and environmental challenges to systems that they power.

Micro-supercapacitors (m-SC) appeared later as another important energy storage unit. Also known as an electrochemical capacitor (EC), a supercapacitor works through the accumulation of the electrostatic charge within an electrochemical double layer at the electrode/electrolyte interface. It could present high specific capacitance, which mainly depends on the high surface area of the electrode materials, or some pseudo-Faradaic charge transfer process. Compared with the batteries, supercapacitors possess inferior energy density but superior power density, i.e., they can be fully charged/discharged in seconds or minutes. Another prominent advantage of supercapacitors is the long cycle life, which is rather comparable with that of the functional devices. For the large-scale application system, supercapacitors are usually used combined with batteries so that both the high energy density of the batteries and the high power density of superapacitors could be utilized to ensure sufficient power supply. Similarly, m-SC is also complementary but indispensable when high power density is required to support the MEMS devices. More importantly, it could even replace the microbatteries when the cycle life of the device is preferred over the energy density for the whole system. As a matter of fact, with the great development of energy harvesters and nanogenerators, i.e., microscaled energy conversion devices that harvest energy from the ambient environment such as solar power, wind, water flow, vibrational energy, and thermal energy from waste heat, m-SC has been much more competitive as an alternative to batteries to play the role of energy storage in the self-powered micro/nanosystems [6]. **Figure 1** illustrates such a sustainable self-powered system, which consists of five different modules, namely energy harvester, energy storage, sensor, data processor/controller, and data transmitter/receiver [7].

M-SC is originally targeted at high power delivery and robust cyclability, and thus, carbon-based electrode materials are first employed to design on-chip electrochemical double-layer capacitors (EDLC), but the capacitance is relatively low [8–10]. The research interest grows quickly since 2010, when several works were reported on the improved design of the carbon electrode materials, especially the carbide-derived carbon film that possesses high volumetric capacitance and compatible with microfabrication [11–13]. Thanks to the fruitful development of the conventional supercapacitors and nanomaterials, m-SCs also received rapid advances when more research groups turn their interest to the on-chip devices, employing various

nanomaterials and designing different fabrication protocols even without being limited to conventional MEMS fabrication routes [14–19].

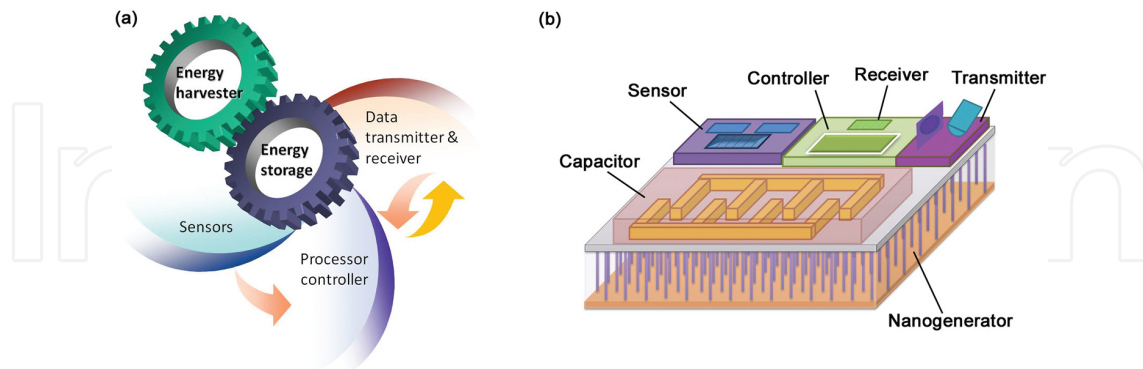


**Figure 1.** (a) Schematic diagram of the integrated self-powered system showing five modules: energy harvester, energy storage, sensors, data processor & controller, and data transmitter & receiver. (b) Prototype of an integrated self-powered system using a nanogenerator as the energy harvester and a capacitor as the storage unit [7].

After several years of active research, the term of micro-supercapacitor is formally defined and the performance metrics are well recognized [6]. According to the definition given by Beidaghi and Gogotsi, micro-supercapacitors, or electrochemical micro-capacitors, refer to miniaturized supercapacitors that are designed and fabricated to serve as power sources or energy storage units in microelectronic devices. Due to the purpose of being specifically assembled to microelectronic devices, there comes the confinement in the fabrication methods that should be compatible with the current techniques in the semiconductor industry. Hence, the general appearance of m-SCs is a device taking up a footprint area in the millimeter or centimeter scale and a thickness of less than 10  $\mu\text{m}$ . The configurations include sandwiched assemblies consisting of thin-film electrodes, planar arrays of microelectrodes like interdigital electrodes, and three-dimensional (3D) architectures of nanoscale building blocks [6, 12]. The former two configurations are commonly adopted in the present laboratory prototypes, while the latter one, 3D architecture, is a composed idea of the next generation whose realization still requires innovations.

## 2. Performance metrics for micro-supercapacitors

As perceived to power the microelectronic devices in a self-powered system, sufficient and energy have to be delivered by the m-SCs. The specific requirement of the power depends on the functional devices varying from environmental sensors to personal electronics, which may be in the range of 1–100  $\mu\text{W}$ . Meanwhile, the duration of the power delivery is also required, meaning certain energy has to be supplied. Thus, power and energy together determine the suitability of an m-SC to power a microelectronic system. It should be mentioned that there is another direction emerging for the application of m-SCs other than micropower units, namely replacing electrolytic capacitors in electronic circuits such as alternating current line filtering.

In order to utilize the advantage of miniaturized size of m-SCs to replace the conventional bulky electrolytic capacitors, the m-SCs have to response fast with a relatively large capacitance, i.e., ideal capacitive behavior with a small resistor-capacitor (RC) time constant (e.g., <8.3 ms for ac line filtering). In such case, the capacitance is a critical parameter for the evaluation, and it is also important whether the capacitance is well kept under faster charge/discharge conditions, which may be termed as rate capability, a terminology from the battery field. In addition, good reversibility (usually assessed by the Coulombic efficiency) and long cycle life should persist for the m-SCs.

As a matter of fact, assuming that an m-SC with a constant capacitance of  $C$  is charged from 0 V to an ultimate voltage of  $U$  in a duration of  $t$ , the stored energy  $E$  is calculated by  $E = 1/2 CU^2$ . And the power  $P$  is calculated by  $P = E/t$ , which is further written as  $P = 1/2 IU$ , if the charge current is  $I$ . Therefore, the energy depends on the capacitance and the voltage. Meanwhile, the power depends on the voltage and the working current that is chosen for the operation of the device. However, the current is not chosen arbitrarily, as the capacitance usually decreases with the increase of current. In other words, the energy shows a declining relation with the power, which is usually described as a Ragone plot. In a word, the performance of an m-SC device could be represented by a Ragone plot, or alternatively, it could be described more intrinsically by the voltage and the capacitance versus the working current. Since the footprint area and the occupied volume are limited for m-SCs when integrated into the system, normalized parameters, i.e., the areal or volumetric energy and power densities and capacitance, are the most important in evaluating the m-SCs. The device performance is determined by the intrinsic properties of the electrode materials, the electrolyte, and the device architecture, wherein the electrode materials play the most critical role and attract abundant studies. In order to compare the properties of different electrode materials effectively, the volumetric energy and power densities as well as the volumetric capacitance should be assessed. This is different from the performance metrics for conventional macro-supercapacitors, where gravimetric capacitance, energy, and power densities are emphasized. Due to the microscaled size, the weight of the electrode materials becomes almost negligible, while the volumetric parameters are the most important concern in developing practical devices. On the other hand, mass density is not a limiting factor, which remarkably expands the choices of the electrode materials for novel m-SCs.

### 3. Electrode materials for micro-supercapacitors

Selection of suitable electrode materials is the kernel in the design of m-SC for certain application. According to the electrochemical energy storage mechanism, the electrode materials currently studied could be divided into three types: carbon-based materials, pseudocapacitive oxides, and conducting polymers. The main purpose of this review is to give a clear comparison among the intrinsic electrochemical properties of the state-of-art electrode materials for m-SC, expecting to open up helpful strategies on developing advanced m-SCs in future.

### 3.1. Carbon-based materials

Carbon is a typical electrode material for EDLC, which possesses good reversibility and cyclability but limited specific capacitance. For conventional supercapacitors, carbon materials are usually fabricated as powders with a loose structure to facilitate the ions diffusion, so as to acquire a high gravimetric capacitance and fast response rate, but the volumetric capacitance is sacrificed. In addition, it is difficult to prepare uniform and qualified thin films from powders, which hinders the direct application of carbonaceous powders in the microelectrodes. Aiming at carbon-based m-SCs, Chimiola et al. tackle the problem by embracing the technological hurdles [12]. They found the carbide-derived carbon (CDC) films produced by selective etching from metal carbides exhibiting an unprecedentedly high volumetric capacity, holding the promise of developing advanced m-SCs. As a first step, they demonstrated that a thin CDC film on a bulk TiC ceramic plate with strong interface adherence was fabricated by direct chlorination at elevated temperatures. Ti is extracted from TiC as  $\text{TiClO}_4$ , forming a porous carbon film, while the conductive TiC plays as both the substrate and the current collector. Both the porosity of the CDC film and the etching speed are closely related to the chlorination temperature [20]. After 15 s etching at  $500^\circ\text{C}$ , a CDC film of  $2\ \mu\text{m}$  thick, with a pore size of about  $0.7\ \text{nm}$ , was synthesized. Its volumetric capacitance reaches  $180$  and  $160\ \text{F}/\text{cm}^3$  in an acetonitrile solution dissolving  $1\ \text{M}$  tetraethylammonium tetrafluoroborate ( $\text{TEABF}_4$ ) and an aqueous solution of  $1\ \text{M}\ \text{H}_2\text{SO}_4$ , respectively, which are contributed by almost pure EDLC. They proposed the fabrication processes for m-SCs based on CDC films, which is schematically shown in **Figure 2**. The deposition of the precursor carbides and gold collectors could be conducted by well-known chemical and physical vapor depositions (CDC and PVD). The chlorination and the plasma etching of the photolithography are well-established techniques. Thus, the good compatibility with the semiconductor industry highlighted the promise of CDC-based m-SC devices.

Heon et al. [21] continued the exploration of the electrochemical property of the CDC films, aiming at the CDC-based m-SCs. The synthesis of uniform and adherent porous CDC films on various substrates by reactive DC magnetron sputtering and chlorination was realized, and the high volumetric capacitance of  $\sim 180\ \text{F}/\text{cm}^3$  in  $1.5\ \text{M}\ \text{TEABF}_4$ /acetonitrile electrolyte was achieved. Later, the on-chip m-SC from CDC films was fabricated and tested by Huang et al. [22]. The preparation process is generally similar to that proposed in **Figure 2a–d** except that Photolithography step is applied on the TiC film to produce interdigitated electrodes before the chlorination and the current collectors deposited on the CDC electrodes are Ti/Au layers instead of the single Au layer. The active material, i.e., TiC-CDC film, was  $1.6\ \mu\text{m}$  thick. The device was dipped into  $1\ \text{M}\ \text{NEt}_4\text{BF}_4$  in propylene carbonate (PC) electrolyte in glove box under Ar atmosphere for electrochemical tests, exhibiting the EDLC behavior over a potential window of  $2\ \text{V}$  with an areal capacitance of  $1.5\ \text{mF}/\text{cm}^2$ , a maximum energy density of  $3.0\ \text{mJ}/\text{cm}^2$ , and a maximum power density of  $84\ \text{mW}/\text{cm}^2$ . At this point, the EDLC property of TiC-CDC film and the feasibility of manufacturing on-chip m-SCs that are to be integrated into MEMS and electronics have been fully demonstrated, which should be recognized as a representative research on the development of carbon-based m-SC device. Nevertheless, the energy and power performance of the TiC-CDC m-SC are within the range of values reported

for other carbon-based micro-supercapacitors, in spite of the high volumetric capacitance of the TiC-CDC active material [10, 22–24]. This is fundamentally attributed to the intrinsic limitation of the capacitance inhibited from the EDLC behavior, which only involves the variation of the ion concentrations in the electric double layer, and the theoretical capacitance is 16–50  $\mu\text{F}/\text{cm}^2$ .

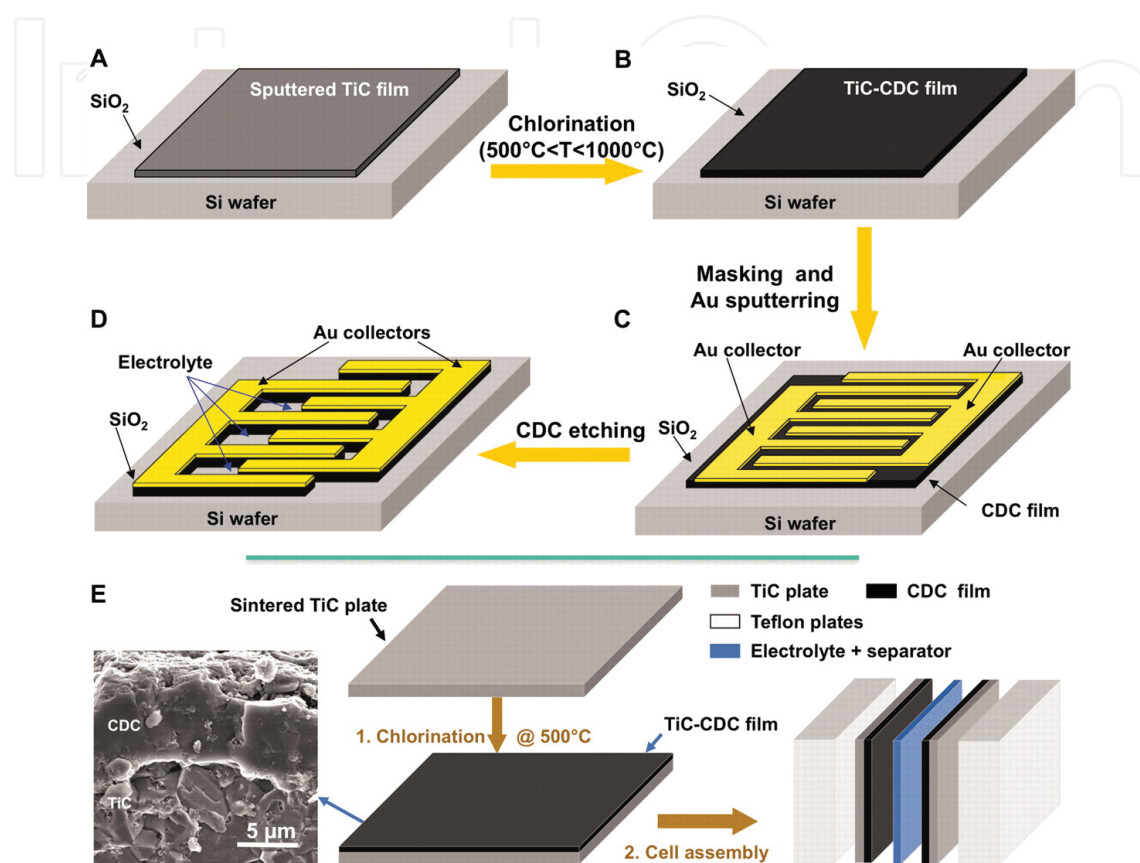


**Figure 2.** (A–D) Schematic of the fabrication of an on-chip m-SC based on the CDC film process, using standard photolithography. (E) Schematic of CDC synthesis and a sandwiched device for electrochemical test. The SEM micrograph shows the interface of CDC/TiC. Reproduced with permission from ref. 12. Copyright (2010) American Association for the Advancement of Science.

To acquire high surface area within the limited electrode volume is still the most effective way to obtain high capacitance for the carbonaceous m-SCs. In this case, activated carbon is still a good choice. However, many well-developed fabrication routes of activated carbon powders are not easily applicable for synthesis of thin activated carbon films (ACFs) which is necessary for m-SCs. The challenges include the formation of cracks in the carbon film due to the shrink of polymers during heating and carbonization, the weak interface between the polymer and the substrate resulted from the large stress produced under the harsh synthesis and cooling conditions, and the possible damage to the brittle film in the photolithographical process. Wei et al reported an effective way to minimize some of the interface stresses in order to fabricate ACFs, namely catalyst-assisted low-temperature carbonization of an organic compound solution [25]. The sucrose and H<sub>2</sub>SO<sub>4</sub> (as a catalyst) aqueous solution was spin-coated onto a silicon wafer, dried at room temperature, carbonized, annealed at 700°C in vacuum to remove

decomposition products of the carbohydrate and catalyst residues, and activated by annealing at 900°C in CO<sub>2</sub> to induce open porosity within carbon. ACFs of 1–2 μm thick were thus produced free of microcracks, while the interface adhesion to the SiO<sub>2</sub>/Si wafer could be reinforced by further annealing at 1100°C in Ar, which could survive lithographical patterning as evidenced experimentally. The electrochemical property of such ACF film electrodes was tested in a symmetric sandwich-type configuration with 1 M H<sub>2</sub>SO<sub>4</sub> as the electrolyte solution. Exhibiting typical EDLC property by the rectangular cyclic voltammetry (CV) curves, an extremely high volumetric capacitance of 390 F/cm<sup>3</sup> was obtained under the slow scan rate of 1 mV/s, which is the highest value reported for carbon film electrode materials at present (see **Figure 3**). Moreover, **Figure 3** shows clearly that the performance was strongly affected by the activation time. As the film becomes more porous after longer activation time, the capacitance increases and the rate capability improves as well, which should be due to easier accessibility of ions into the films. It means that the volumetric metrics of the carbonaceous electrode materials could be greatly enhanced when the materials structure is carefully optimized with proper fabrication techniques. But it is also worth noting that the fabrication process is still quite harsh as several times of high temperature annealing are required, which probably causes difficulties for the practical manufacturing of the devices integrated on the chips, although the realization of uniform and robust ACF films represents a great progress itself.

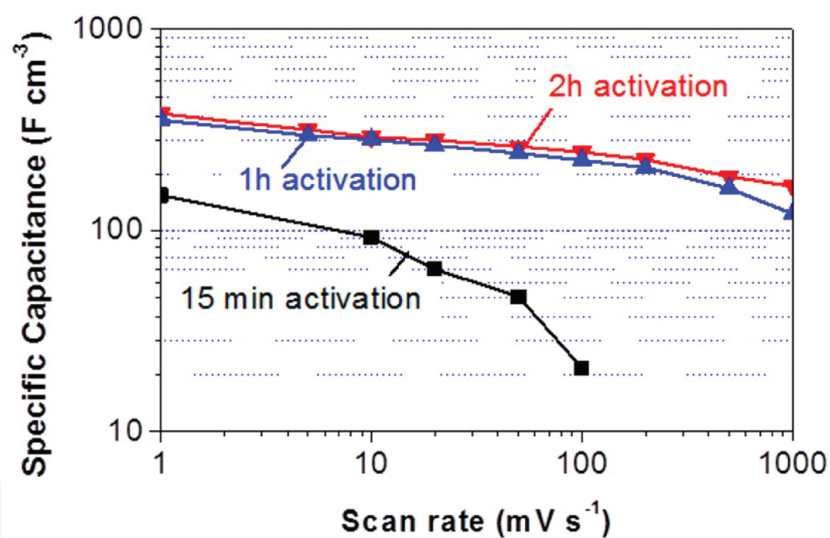


**Figure 3.** Rate performance of symmetric ACF electrode cells in 1 M H<sub>2</sub>SO<sub>4</sub> electrolyte: volumetric capacitance of ACFs as a function of CV scan rate. Reproduced with permission from ref. 25. Copyright (2013) American Chemical Society.

As a matter of fact, there have also been great advances in the research of carbon-based electrode materials for macro-scaled supercapacitors that pursue higher volumetric property in recent years. For example, liquid-mediated dense graphenes [26] and nitrogen-doped mesoporous carbon [27] were reported to have unprecedentedly high volumetric capacitance that is comparable with pseudocapacitive materials. Pseudocapacitance has been induced on these modified carbon materials actually [28]. Yang et al. tackle the problem by considering the paradox between gravimetric capacitance  $C_{wt}$  and packing density of the carbon  $\rho$  [26]. The



specific volumetric capacitance  $C_{\text{vol}}$  is simply calculated by  $C_{\text{vol}} = C_{\text{wt}} \times \rho$ , while  $C_{\text{wt}}$  is always compromised with the increase of  $\rho$ . They addressed this challenge with liquid electrolyte-mediated chemically converted graphene (EM-CCG) films. They started with the chemically reduced graphene oxide, namely chemically converted graphene (CCG) sheets, which are well dispersed in water and could self-assemble to form an oriented hydrogel film through a directional flow-induced bottom-up assembly process. With the CCG sheets remaining largely separated, a high  $C_{\text{wt}}$  of over 200 F/g was obtained, while the packing density was only  $\sim 0.069 \text{ g/cm}^3$ , resulting in a mediocre  $C_{\text{vol}}$  of  $\sim 18 \text{ F/cm}^3$ . In order to compress the CCG hydrogel films, they were exchanged with a miscible mixture of volatile and nonvolatile liquids and then subjected to removal of the volatile liquid by vacuum evaporation. As a consequence, the film thickness was reduced, while the sheets remained solvated by the nonvolatile liquid (e.g., sulfuric acid). Through electrochemical tests in 1 M  $\text{H}_2\text{SO}_4$  electrolyte, they found that the  $C_{\text{vol}}$  of the EM-CCG films was nearly proportional to  $\rho$ , and the highly compact one with  $\rho$  of  $1.33 \text{ g/cm}^3$  yielded a  $C_{\text{vol}}$  of  $255.5 \text{ F/cm}^3$  at  $0.1 \text{ A/g}$ , which is much higher than previous porous carbon materials for conventional SCs. Although the adaptable intersheet spacing among the graphene sheets is particularly emphasized in this work to optimize the  $C_{\text{vol}}$ , other factors such as surface wettability and the pore interconnectivity are also important to realize superior capacitive property for the carbon materials [28]. In other words, both surface chemical property and structural configuration play significant roles in determining the volumetric capacitance of the carbonaceous electrode materials. Lin et al. made a breakthrough in the chemical way, finding that a nitrogen-doped ordered mesoporous few-layer carbon has an extremely high specific capacitance of  $855 \text{ F/g}$  when tested in  $0.5 \text{ M H}_2\text{SO}_4$  electrolyte at  $1 \text{ A/g}$  (comparing with the  $200 \text{ F/g}$  for the CCG sheets) [27]. The extra capacitance comes from the pseudocapacitance contributed by the doped N in the pyrrolic and pyridine sites incorporating protons. To be assembled into supercapacitors, they studied variation in the volumetric capacitance with the mass loading of this N-doped mesoporous carbon materials, which showed that the highest value of  $560 \text{ F/cm}^3$  was reached at the loading of  $6 \text{ mg/cm}^2$ . Although great advances have been accomplished in the carbonaceous materials for the macro-scaled SCs, they are in the form of either self-standing membranes or powders, difficult to be integrated into the on-chip m-SCs.

Besides the attempts to enhance the volumetric capacitance for energy storage through a proper film fabrication process, there is another important direction for carbon-based m-SC, i.e., to utilize its fast response rate to replace electrolytic capacitors by making open-structured devices [29, 30]. Pech et al. produced m-SCs through electrophoretic deposition of a several-micrometre-thick layer of nanostructured carbon onions (OLC) with diameters of  $6\text{--}7 \text{ nm}$  onto the interdigital Au current collectors patterned on silicon wafers. The OLC particles were prepared by annealing nanodiamond powder at  $1800^\circ\text{C}$ . A stable capacitive behavior was obtained for the microdevice over a  $3 \text{ V}$  potential window in a  $1 \text{ M}$  solution of tetraethylammonium tetrafluoroborate in PC, with a linear dependence of the discharge current on the scan rate and low resistive contributions up to  $100 \text{ V/s}$ , which is about three orders of magnitude higher than conventional SCs. Such a microdevice preserves an areal capacitance of  $0.9 \text{ mF/cm}^2$  at  $100 \text{ V/s}$ , which is comparable to values usually reported at much lower scan rates ( $1\text{--}100 \text{ mV/s}$ ) for microscaled EDLC devices ( $0.4\text{--}2 \text{ mF/cm}^2$ ) [9, 11, 31]. The most appealing

feature of such OLC m-SC is the extremely small characteristic relaxation time constant  $\tau_0$  (the minimum time needed to discharge all the energy from the device with an efficiency of greater than 50%), which is only 26 ms, much lower than that of the AC-based microdevice ( $\tau_0 = 700$  ms) or OLC-based macroscopic devices ( $\tau_0 > 1$  s) [32]. **Figure 4** shows the Ragone plot of several typical energy storage devices designed for power microelectronics applications, including a 500- $\mu$ Ah thin-film lithium battery, a 25-mF supercapacitor, and an electrolytic capacitor of the same absolute capacitance, as well as the m-SCs composed of AC, OLC and graphene-based materials. It could be seen that the power density of the OLC-based m-SC has reached that of the electrolytic capacitors, but the energy density is more than one order of magnitude higher than that of latter.

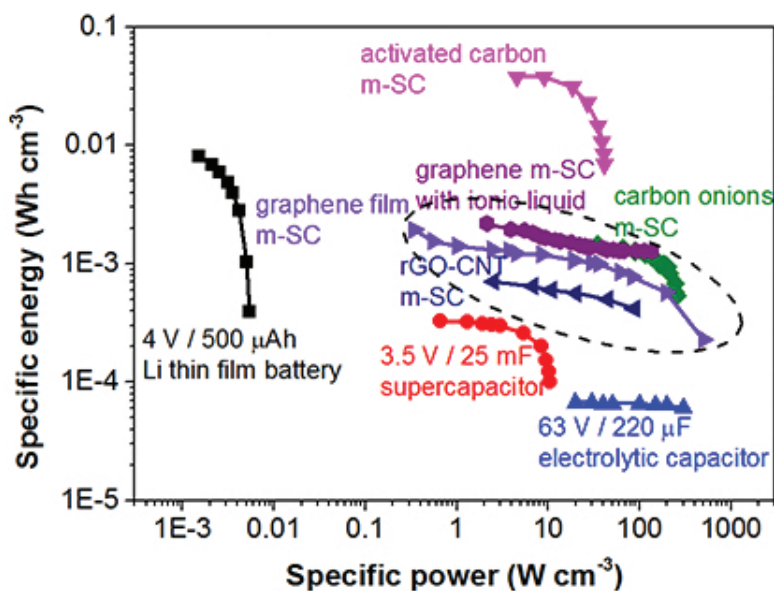


**Figure 4.** A Ragone plot showing the relationship between the volumetric energy density and power density of typical electrolytic capacitors, supercapacitors, batteries, and the m-SCs with AC and OLC electrode [29], as well as the m-SCs with various graphene films [17, 33] and graphene-CNT (rGO-CNT) composite electrode materials [34]. The dashed ellipsoid generally describes the best high power performance currently achieved by these state-of-art m-SCs assembled with conductive carbon electrode materials.

Thereafter, several research papers reported high-power m-SCs fabricated from graphene, whose performance reaches a similar level with that of the OLC-based device (see **Figure 4**). For example, interdigitated graphene m-SCs were produced through laser burning along designed patterns on a graphene oxide (GO) film supported on a PET sheet which was inserted into a LightScribe DVD drive [17]. Due to the photo-thermal effect under laser radiation, the exposed GO was converted into graphene, constructing the positive and negative electrodes, while the unexposed GO remained insulating and served as a separator. A hydrogel-polymer electrolyte, poly(vinyl alcohol) (PVA)-H<sub>2</sub>SO<sub>4</sub>, was then drop-cast on the patterned area to create a planar m-SC. Such a device using reduced GO (rGO) as electrode materials exhibits an areal capacitance of 2.32 mF/cm<sup>2</sup> and a volumetric capacitance of 3.05 F/cm<sup>3</sup>, with a characteristic relaxation time of only 19 ms and a high power density of nearly 200 W/cm<sup>3</sup>. There is another planar device using rGO and carbon nanotube (CNT) composites as the electrode material,

which is prepared by combining electrostatic spray deposition (ESD) and photolithography lift-off methods [33]. The m-SC delivers an areal capacitance of  $6.1 \text{ mF/cm}^2$  at  $10 \text{ mV/s}$ , and a value of  $2.8 \text{ mF/cm}^2$  is still preserved at  $50 \text{ V/s}$ , corresponding to  $3.1 \text{ F/cm}^3$ . Its characteristic time constant is only  $4.8 \text{ ms}$ . An even faster m-SC device is made from graphene films of only  $6\text{--}100 \text{ nm}$  thick, whose maximum capacitance is  $0.807 \text{ mF/cm}^2$  and  $17.9 \text{ F/cm}^3$  (specific values of  $0.323 \text{ mF/cm}^2$  and  $71.6 \text{ F/cm}^3$  for the electrode material), with the maximum power density reaching  $495 \text{ W/cm}^3$ , the maximum energy density  $2.5 \text{ mWh/cm}^3$ , and the characteristic time constant as short as  $0.28 \text{ ms}$  [34]. It is concluded from these researches that the electronic conductivity of the electrodes has to be enhanced in order to acquire fast response performance. The most straightforward route is to reduce micropores within the electrodes and enlarge the open area in direct contact with the electrolyte, as the outmost surface is the most easily accessible with the ions for charge/discharge processes. However, such a design is usually at the cost of volumetric capacitance, and the film thickness should be thin as well, which thus limits the areal capacitance of the device.

### 3.2. Pseudocapacitive oxides

For the pseudocapacitive materials, Faradaic charge transfer occurs on the electrode/electrolyte interface during charge/discharge processes, giving much higher areal capacitance than EDLC does. Many transition metal oxides exhibit pseudocapacitive behavior in certain aqueous electrolyte.  $\text{RuO}_2$  is the first discovered pseudocapacitive oxide and still the most ideal candidate [35, 36]. Within the potential range of  $0\text{--}1.4 \text{ V}$  vs. SHE,  $\text{RuO}_2$  continuously changes its valence from  $\text{Ru}^{2+}$  to  $\text{Ru}^{4+}$ , following the reaction of  $\text{RuO}_2 + x\text{H}^+ + xe^- \leftrightarrow \text{RuO}_{2-x}(\text{OH})_x$ , where  $0 \leq x \leq 2$  [37]. The process undergoes through both electron transfer and proton incorporation in  $\text{RuO}_2$  particles. Because of the good electronic conductivity and proton conductivity for hydrated  $\text{RuO}_2$ , fast and reversible charge/discharge pseudocapacitance according to adsorption isotherm model [38] is observed, with a specific capacitance value over  $600 \text{ F/g}$ . The practical capacitance is closely related to the crystallinity of the material. For crystalline  $\text{RuO}_2$ , protons only adsorb on the surface instead of entering the grains, which provides a capacitance per real surface area of  $339\text{--}490 \mu\text{F/cm}^2$  and an overall specific capacitance of about  $380 \text{ F/g}$  [37]. For amorphous  $\text{RuO}_2 \cdot x\text{H}_2\text{O}$ , protons could easily transport inside the domains, thus presenting a much higher specific capacitance.

There have been researches on  $\text{RuO}_2$  thin-film electrodes ever since 1990s. Jow and Zheng coated an amorphous  $\text{RuO}_2$  film onto Ti substrate through sol-gel method. In spite of inferior uniformity and many cracks, the film still shows a capacitance of  $40 \text{ mF/cm}^2$  as tested at  $50 \text{ mV/s}$  in  $0.5 \text{ M H}_2\text{SO}_4$ , which decreases by only  $10\%$  at  $500 \text{ mV/s}$  [37]. Zheng et al. further employed pulsed laser deposition (PLD) to prepare the  $\text{RuO}_2$  films [37]. The amorphous film deposited at room temperature possessed the highest capacitance ( $6.3 \text{ mF/cm}^2$ ). As the deposition temperature increased to above  $200^\circ\text{C}$ , the capacitance reduced to only  $0.3 \text{ mF/cm}^2$ . The diffusion length of protons in amorphous  $\text{RuO}_2$  film was estimated to be about  $5.8 \text{ nm}$ , while it reached  $>11.1 \text{ nm}$  in  $\text{RuO}_2 \cdot x\text{H}_2\text{O}$ . Assuming the diffusion coefficient to be  $>10^{-8} \text{ cm}^2/\text{s}$ , the proton in and out diffusion from  $\text{RuO}_2$  film is in the order of  $10 \mu\text{s}$  for a diffusion length less than  $11.1 \text{ nm}$ . This explains the good rate capability of the  $\text{RuO}_2$  electrode (i.e., it

could be charged/discharged at a rate of over 500 mV/s without loss of the capacitance). Thus, for the RuO<sub>2</sub> electrode, the charge/discharge rate is mainly limited by the electric resistance and the proton transport in the electrolyte, rather than the proton diffusion inside the RuO<sub>2</sub> material.

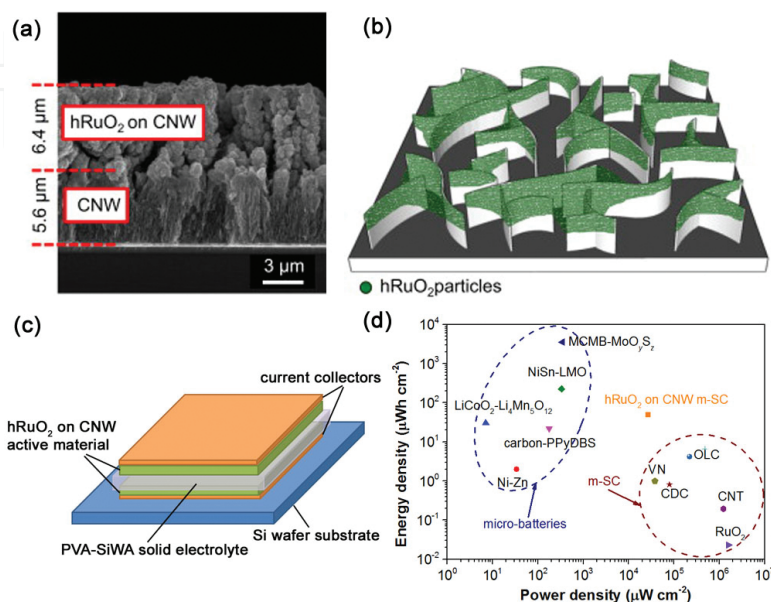


**Figure 5.** (a) Cross-section SEM image of a CNW film (bottom) electrodeposited by hRuO<sub>2</sub> on its top. (b) Schematic of the vertically aligned CNW decorated with hRuO<sub>2</sub> particles. (c) Schematic diagram of on-chip m-SC with 2D architecture. (d) A Ragone plot showing the energy and power density of the CNW/hRuO<sub>2</sub>-based m-SC, compared with other advanced m-SCs and microbatteries. Reproduced with permission from ref. 39. Copyright (2014) Elsevier Ltd.

The development of RuO<sub>2</sub>-based m-SCs emerged in recent years. Liu et al. [36] fabricated the planar device through depositing RuO<sub>2</sub> nanorods onto the patterned stack layer of Ru/Au/Ti/SiO<sub>2</sub> on silicon wafer, which was subjected to electrodeposition for another layer of hydrous RuO<sub>2</sub> on top. It worked well in 0.5 M H<sub>2</sub>SO<sub>4</sub> electrolyte, providing a capacitance of 21.4 mF/cm<sup>2</sup> at 50 mV/s and 14.9 mF/cm<sup>2</sup> at 500 mV/s. Makino et al. [18] reported the fabrication of an m-SC with ordered mesoporous RuO<sub>x</sub> as the electrode material, which was produced by controlled electro-deposition using a lyotropic liquid crystal template method and subsequent electro-oxidation on an interdigital electrode array. The device exhibited good capacitive property with maximum capacitance of 12.6 mF/cm<sup>2</sup> and maximum energy of 1.49 μWh/cm<sup>2</sup> at the slowest discharge rate of 0.38 mA/cm<sup>2</sup> and maximum power delivery of 750 μW/cm<sup>2</sup> at 2.88 mA/cm<sup>2</sup>. More recently, a new m-SC device based on hydrous RuO<sub>2</sub>/carbon nanowalls hierarchical structured composite electrode was proposed by Dinescu et al., which showed an exceptionally high capacitance [39]. Carbon nanowalls (CNW), or vertically oriented graphene sheets, is a good EDLC material with a large surface area, good electronic conductivity, and excellent chemical stability, while RuO<sub>2</sub> is an ideal pseudocapacitive materials with a high specific capacitance. A silicon wafer coated with an insulating Si<sub>3</sub>N<sub>4</sub> layer was first deposited with a 40 nm Cr/200 nm Pt layer by evaporation as the current collector and subjected to the CNW layers growth by PECVD at 700°C, and then, electrodeposition of hydrous RuO<sub>2</sub>

(hRuO<sub>2</sub>) onto the CNW was carried out afterwards, after which the samples were annealed in air at 150 °C. The pristine CNW layer is 12 μm thick, with a capacitance of 5.7 mF/cm<sup>2</sup> in 0.5 M H<sub>2</sub>SO<sub>4</sub> electrolyte, close to the values of other carbonaceous electrodes. When about half of the CNW layer was decorated with hRuO<sub>2</sub> (see **Figure 5a, b**), the hybrid electrode exhibited an extremely high capacitance of 1094 mF/cm<sup>2</sup> at 2 mV/s, which is three orders of magnitude higher than that of the state-of-the-art graphene-based m-SCs [34], and also far larger than most other advanced m-SC electrodes [22, 25, 33, 40]. An all-solid-state m-SC in a stack configuration was realized with a solid-polymer electrolyte sandwiched between two CNW/hRuO<sub>2</sub> electrodes (see **Figure 5c**), delivering an energy density of 49 μWh/cm<sup>2</sup>, i.e., 20 mWh/cm<sup>3</sup>. Such a value is even comparable to the state-of-the-art lithium ion microbatteries [41–43], but its power density and cycle life (more than 90% is retained after 2000 cycles) are much higher than that of the latter, which is shown in **Figure 5d**.

In spite of the ideal pseudocapacitive property, RuO<sub>2</sub> is too expensive for large-scale application. Cheaper oxides have been widely researched, such as MnO<sub>2</sub> and NiO, wherein MnO<sub>2</sub> attracts the most attention [44, 45]. MnO<sub>2</sub> works in neutral aqueous solutions, with the potential window within 0.8 V and above 0 V vs. Ag/AgCl, and thus is suitable to serve as a positive electrode in asymmetric devices. Its working mechanism is the surface adsorption/desorption of the electrolytic cations and protons in the solution, which is described as the reaction  $\text{MnO}_2 + x\text{C}^+ + y\text{H}^+ + (x+y)\text{e}^- \leftrightarrow \text{MnOOC}_x\text{H}_y$ . [46, 47]. It is obvious from the CV curve on **Figure 6** that the charge/discharge behavior of MnO<sub>2</sub> is similar to that of EDLC. Besides, the abundant resource and the safe working condition of neutral solutions also boost the wide research on MnO<sub>2</sub>, although the specific capacitance of MnO<sub>2</sub> powders or micrometer-thick films is only 150 F/g.

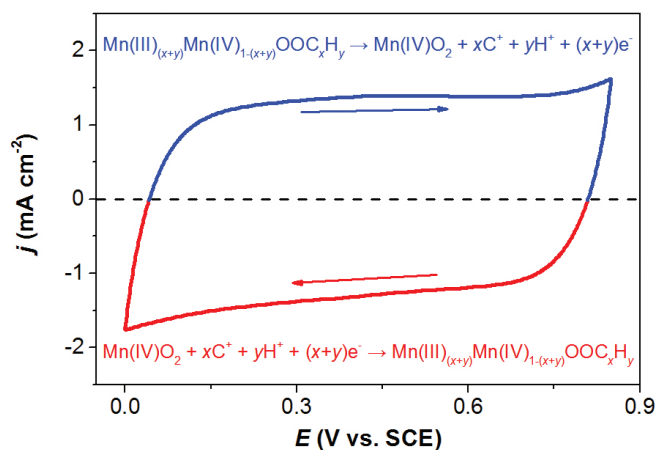


**Figure 6.** The CV curve of MnO<sub>2</sub> electrode tested in 2 M Li<sub>2</sub>SO<sub>4</sub> aqueous electrolyte solution..

The intrinsic electrochemical properties of MnO<sub>2</sub> films produced by different preparation conditions and of different morphologies and structures have been explored [48–51]. For example, the MnO<sub>2</sub> film deposited by cathodic electrodeposition is poorly crystalline and porous, whose specific capacitance strongly decreases with the scan rate and the film thick-

ness [51]. The specific capacitance of a film bearing a deposited mass of 45  $\mu\text{g}/\text{cm}^2$  is tested to be 353 F/g (15.9  $\text{mF}/\text{cm}^2$ ) at 2 mV/s and 135 F/g (6.1  $\text{mF}/\text{cm}^2$ ) at 100 mV/s. For films annealed under 200  $^\circ\text{C}$ , whose porosity is reduced and crystallinity increased, the maximum specific capacitance is decreased, while rate capability is improved more or less. PLD has also been utilized to prepare manganese oxide films, with amorphous  $\text{MnO}_x$ , crystalline  $\text{Mn}_2\text{O}_3$ , and  $\text{Mn}_3\text{O}_4$  to be produced under different deposition temperatures and the partial pressure of oxygen [50]. The crystalline  $\text{Mn}_2\text{O}_3$  film possesses the highest specific capacitance, 210 F/g at 1 mV/s for a film of 120 nm, while the  $\text{Mn}_3\text{O}_4$  film has the lowest value.

Because of the insulating property of  $\text{MnO}_2$  and the increased difficulty for ions to access into a thicker film, the rate capability of  $\text{MnO}_2$  film is always unsatisfying. Research efforts have been devoted to enhance the electronic conductivity so as to improve the rate capability. Si et al. [52] deposited the  $\text{MnO}_x/\text{Au}$  multilayer film, which showed a capacitance of 32.8  $\text{F}/\text{cm}^3$ , higher than that of the pure  $\text{MnO}_x$  film electrode (19.9  $\text{F}/\text{cm}^3$ ). Two kinds of interdigital m-SCs were prepared using these two films. The device of  $\text{MnO}_x/\text{Au}$  multilayer possessed a smaller equivalent series resistance (ESR) and a shorter characteristic relaxation time (5 ms). Doping is another way to adjust the electrochemical property. By doping Mo into the electrodeposited manganese oxide, a film of  $\text{MnMo}^{6+}_{0.18}\text{O}_{1.18}(\text{OH})_{0.59}(\text{H}_2\text{O})_{0.25}$  was obtained, whose specific capacitance (190.9 F/g and 18.5  $\text{mF}/\text{cm}^2$  at 5 mV/s), cycling reversibility, and rate capability were all improved as compared with the undoped film [53]. It was found that the electronic resistivity of a  $\sim 0.5\text{-}\mu\text{m}$ -thick film was reduced from  $5.0 \times 10^4$  to  $3.0 \times 10^1 \Omega \text{ cm}$  after being doped with Mo, which suggested that the enhancement of the electrochemical property is mainly attributed to the increase in electronic conductivity. Similar effect was also discovered in doping Co into the electrodeposited manganese oxide film and in doping V into the PLD-deposited amorphous manganese oxide film [54, 55].

Other pseudocapacitive oxides include  $\text{Co}_3\text{O}_4$ , NiO,  $\text{NiCo}_2\text{O}_4$ , and so on [56–58]. They could reversibly form hydroxides in alkaline solutions, the process of which could be represented as  $\text{M}_3\text{O}_4 + \text{OH}^- + \text{H}_2\text{O} \leftrightarrow 2\text{MOOH} + \text{e}^-$ , wherein M refers to elements such as Ni and Co. Their specific capacitances are reported to be very high (382–1400 F/g); however, phase transformations are always involved during the reaction processes, and the charge/discharge behaviors are more like that of batteries, for example, with potential plateaus, short potential windows (0.4–0.5 V), limited rate capabilities [56].

Overall, pseudocapacitive oxides could exhibit high specific capacitance, but poor rate capability and cycling stability hinder their application, which is mainly attributed to their insulating property. For the film electrodes, when thickness increases, the areal capacitance rarely scales up as expected. To disperse the active materials onto a 3D current collector is a common way to acquire certain areal capacitance with acceptable rate capability, which relies on the innovation of nanofabrication techniques. Nevertheless, the intrinsic relationship between the comprehensive electrochemical property and the microstructure of the oxides is still worth studying, which may help to optimize the intrinsic electrochemical performance of the film electrodes, contributing to the development of m-SCs compatible with conventional microelectronics manufacturing techniques.

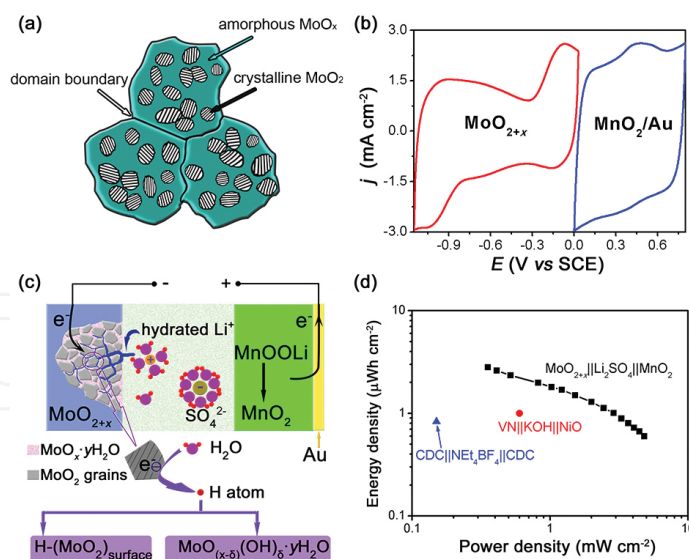


**Figure 7.** (a) Schematic of the multi-phased microstructure of the  $\text{MoO}_x$  film deposited at  $150^\circ\text{C}$  by magnetron sputtering. (b) CV curves of  $\text{MoO}_{2+x}$  and  $\text{MnO}_2$  films in 2 M  $\text{Li}_2\text{SO}_4$  electrolyte, at 50 mV/s. (c) Illustrative diagram for the working process and (d) a Ragone plot showing energy density vs. power density of  $\text{MoO}_{2+x}(-)//2\text{ M Li}_2\text{SO}_4//\text{MnO}_2(+)$  microdevice. The performances of representative m-SCs of EDLC type (symmetric device based on CDC electrode [22]) and other pseudocapacitive type (asymmetric device based on VN and NiO electrodes [61]) are also plotted for reference [59, 60] Reproduced with permission from ref. 60. Copyright (2014) Elsevier Ltd.

Our group has systematically studied the fabrication and electrochemical property of molybdenum oxide thin film, which has various chemical valences with quite different properties [59]. The composition, microstructure, and morphology were controlled to enhance the electrochemical performance of the molybdenum oxide film, and its potential to be applied as a superior electrode material in m-SC is evaluated. We fabricated electronically conductive  $\text{MoO}_{2+x}$  films via RF magnetron sputtering from a  $\text{MoO}_3$  target. Multi-valence composition and mixed-phased microstructure, i.e., coexistence of  $\text{MoO}_2$  nanocrystals and amorphous  $\text{MoO}_x$  ( $2 < x \leq 3$ ), were acquired in these films (see **Figure 7a**), which exhibit excellent pseudocapacitance in  $\text{Li}_2\text{SO}_4$  electrolyte [59]. The  $\text{MoO}_x$  ( $x \approx 2.3$ ) film deposited at  $150^\circ\text{C}$  presented an areal capacitance of  $31\text{ mF}/\text{cm}^2$  at  $5\text{ mV}/\text{s}$ , corresponding to a volumetric value of  $392\text{ F}/\text{cm}^3$ , superior to most of the advanced m-SC electrode materials previously discussed. Forty-seven percent of the capacitance was retained when the scan rate increases from 20 to  $500\text{ mV}/\text{s}$ , meaning good rate capability. The cycling stability is excellent as well, with 100% preserved after 5000 cycles. The multi-phased microstructure of such  $\text{MoO}_x$  films is quite interesting, as it intrinsically endows the material with superior electrochemical property. The pseudocapacitance originates from the cation ( $\text{H}^+$  and  $\text{Li}^+$ ) insertion/extrusion in the amorphous  $\text{MoO}_x$ , in which  $\text{H}^+$  is more active. The  $\text{MoO}_2$  grains could also catalyze the decomposition of water combined on the surface, producing H atoms that could be reversibly stored in amorphous  $\text{MoO}_x$  and thus promote the pseudocapacitive process. Furthermore, the crystalline  $\text{MoO}_2$  also improves the electronic conductivity and maintains a stable structure of the film [60]. Another interesting feature about  $\text{MoO}_x$  film is its relatively negative potential window, i.e., between  $-1.1$  and  $0\text{ V}$  vs. SCE, which makes it a proper anode material relative to other pseudocapacitive oxides. Thus, an asymmetric microdevice of  $\text{MoO}_{2+x}(-)//2\text{ M Li}_2\text{SO}_4//\text{MnO}_2(+)$  is successfully fabricated.

It could be seen from **Figure 7b** that the working potential windows of the two electrodes well complement to each other. The working mechanism is described in the schematic of **Figure 7c**. A high energy density of  $2.8 \mu\text{Wh}/\text{cm}^2$  at a real power density of  $0.35 \text{ mW}/\text{cm}^2$  was obtained from this device, combined with good stability (no capacitance loss for 10,000 cycles). The Ragone plot of **Figure 7d** shows that the performance of this asymmetric device is much better than other typical state-of-art m-SCs.

Microelectrode <sup>a</sup>	Set up	Thickness	$C_V$ ( $\text{F cm}^{-3}$ ) <sup>b</sup>	$\tau_c$ (ms)	Cyclability	References
Activated carbon	Two-electrode assembly in 1 M $\text{H}_2\text{SO}_4$	1.5 $\mu\text{m}$	390 ( $1 \text{ mV s}^{-1}$ )	1111	95% after 10,000 cycles at $10 \text{ A g}^{-1}$	[25]
TiC-CDC nanofelts	Filled into a micro cavity electrode tested in 1 M $\text{H}_2\text{SO}_4$	125 $\mu\text{m}$ in diameter, 35 $\mu\text{m}$ in depth	12 ( $10 \text{ mV s}^{-1}$ )	379	Stable over 10,000 cycles	[64]
Polyaniline nanowire arrays	Interdigital micro device with $\text{H}_2\text{SO}_4$ -PVA gel	400 nm	588 ( $0.1 \text{ mA cm}^{-2}$ )	–	96% after 1000 cycles	[16]
rGO-CNT composite	Interdigital micro device with 3 M KCl	6 $\mu\text{m}$	37.5 ( $10 \text{ mV s}^{-1}$ )	4.8	Slight decline over 1000 cycles	[33]
rGO	Interdigital micro device with $\text{H}_3\text{PO}_4$ /PVA gel	25 nm	359 ( $1 \text{ A g}^{-1}$ )	–	90% after 1000 cycles	[65]
Photoresist-derived porous carbon	Three-electrode assembly in 3.5 M KCl	1 $\mu\text{m}$	35 ( $10 \text{ mV s}^{-1}$ )	–	No loss after 10,000 cycles at $100 \text{ mV s}^{-1}$	[66]
TiC-CDC	Three-electrode assembly in 1 M $\text{H}_2\text{SO}_4$ or 1 M $\text{TEABF}_4$	~2 $\mu\text{m}$	160 (in $\text{H}_2\text{SO}_4$ ); 180 (in $\text{TEABF}_4$ )	–	–	[12]
$\text{MnO}_x/\text{Au}$ multilayers	Interdigital micro device with $\text{H}_2\text{SO}_4$ -PVA gel or 1 M $\text{Li}_2\text{SO}_4$	50 nm	78.6 ( $10 \text{ mV s}^{-1}$ , $\text{H}_2\text{SO}_4$ -PVA gel); ~400 ( $10 \text{ mV s}^{-1}$ , $\text{Li}_2\text{SO}_4$ )	5	74.1% retained after 15,000 cycles at $1 \text{ V s}^{-1}$	[52]
rGO	Interdigital microdevice with $\text{H}_2\text{SO}_4$ /PVA gel	15 nm	71.6 ( $10 \text{ mV s}^{-1}$ )	0.28	98.3% retained after $10^5$ cycles at $50 \text{ V s}^{-1}$	[34]
CNT film	Three-electrode assembly in 1 M $\text{H}_2\text{SO}_4$	30–250 nm	$132 \pm 8$ ( $50 \text{ mV s}^{-1}$ )	–	–	[67]
Laser-scribed graphene	Interdigital microdevice with $\text{H}_2\text{SO}_4$ -PVA gel	7.6 $\mu\text{m}$	~12.2 ( $10 \text{ mV s}^{-1}$ )	19	94% retained after 10,000 cycles	[17]
Onion-like carbon	Interdigital microdevice in 1 M $\text{Et}_4\text{NBF}_4/\text{PC}$	7 $\mu\text{m}$	~9.7 ( $1 \text{ V s}^{-1}$ )	26	Stable over 10,000 cycles at $10 \text{ V s}^{-1}$	[29]
Activated carbon	Interdigital microdevice in 1 M $\text{Et}_4\text{NBF}_4/\text{PC}$	5 $\mu\text{m}$	~92.8 ( $500 \text{ mV s}^{-1}$ )	700	–	[29]
Electrodeposited $\text{MoO}_x$	Three-electrode assembly in 2 M $\text{Li}_2\text{SO}_4$	120 nm	1162 ( $5 \text{ mV s}^{-1}$ )	1381	88% retained after 4000 cycles at $100 \text{ mV s}^{-1}$	[62]
Electrodeposited $\text{MoO}_x$ after annealing at $350^\circ\text{C}$ for 1.5 h	Three-electrode assembly in 2 M $\text{Li}_2\text{SO}_4$	63 nm	700 ( $5 \text{ mV s}^{-1}$ )	11	99% retained after 4000 cycles at $100 \text{ mV s}^{-1}$	[62]

<sup>a</sup>Carbide-derived carbon (CDC), reduced graphene oxide (rGO), carbon nanotubes (CNT).

<sup>b</sup>Please note that  $C_V$  here corresponds to the electrodes, and some of the values are read from the reported plots, or estimated from the cell data.

**Table 1.** Electrochemical properties of typical m-SC microelectrodes in literature [62].



The pseudocapacitive  $\text{MoO}_x$  film was further prepared by electrodeposition, with its electrochemical property adjusted by annealing under different conditions [62]. Optimal experimental parameters were determined to fabricate the film containing  $\text{MoO}_2$  nanocrystallites and amorphous  $\text{MoO}_x$ . A film of 63 nm thick exhibited a high volumetric capacitance of  $700 \text{ F/cm}^3$ , good rate capability with a relaxation time constant of 11 ms, and excellent cycling stability of 99% capacitance retention after 4000 cycles. The performance is superior to other typical microelectrodes for m-SCs, the comparison of which is listed in **Table 1**. Furthermore, a 3D microelectrode was developed by electrodepositing  $\text{MoO}_x$  on a Ti nanorod array prepared by oblique angle deposition [63]. An areal capacitance of  $27 \text{ mF/cm}^2$ , corresponding to a high volumetric capacitance of  $643 \text{ F/cm}^3$ , was obtained as well as satisfying cycling stability, which is rather attractive compared to other 3D microelectrodes. And post-annealing in reductive atmosphere improved its rate capability and response speed. Thus, the further improvement in electrochemical property of  $\text{MoO}_x$  electrode by architecture design of employing current collectors with large specific area promotes its practical application in m-SCs.

### 3.3. Conducting polymers

Conducting polymers are another group of pseudocapacitive materials, which work through the fast redox reaction of ion doping [68, 69]. Currently studied conducting polymers mainly include P-type doping materials such as polypyrrole (PPy) and polyaniline (PANI), and N-type doping materials such as polythiophene (PTH). They are electronically conductive, leading to low ESR, and their capacitance is generally 2–3 times as high as that of activated carbon materials. However, the cycling stability is always unsatisfying due to the large volume expansion and shrink during the charge/discharge processes. The application of conducting polymers in m-SCs is relatively pioneering, i.e., developed in 3D structures [16, 70, 71]. Beidaghi and Wang [71] fabricated such a 3D-structured interdigital m-SC through carbon-microelectrochemical system (C-MEMS) technology. Briefly, the carbonization of patterned photoresist pillars produced microarrays of carbon pillars on the interdigital carbon layer supported on silicon wafer. The carbon arrays served as the C-MEMS current collectors, on which PPy was coated by electrodeposition. The resulted PPy/C-MEMS electrode presented a high areal capacitance of  $162 \text{ mF/cm}^2$  (volumetric capacitance estimated to be  $11.6 \text{ F/cm}^3$ ) and a power density of  $1.62 \text{ mW/cm}^2$  at  $20 \text{ mV/s}$  scan rate. Correspondingly, the entire symmetric m-SC device exhibited an average capacitance of  $78 \text{ mF/cm}^2$  and a power density of  $0.63 \text{ mW/cm}^2$ . In spite of the high areal capacitance, the electrodes were not robust for consecutive cycling, as only 56% of the capacitance is retained after 1000 cycles.

## 4. Summary

Architecture design is especially important for m-SC, which significantly affects the comprehensive device performance. Structure of a separator layer sandwiched by thin-film electrodes is the traditional architecture, but the performance is closely related to the thickness of the electrode layer, which hinders it from scaling up to acquire higher areal energy density [12]. In-plane interdigital architecture is often employed in recent years, especially for fast response

devices [13, 17]. Besides, integrated 3D architectures have also been proposed for m-SCs [19]. The microelectrodes with the structure of micro- or nanoarrays as cited above [16, 63, 70, 71] could be considered as ordered 3D structure, which is already realized by microfabrication techniques. However, a “true” 3D device is composed to consist of interpenetrating electrodes that are separated by a very thin layer of electrolyte, which is proposed by Long and coworkers [5]. Although several possible strategies for fabrication of electrochemical energy storage devices with 3D architectures have been proposed [72], there has been no work fully realized the concept of 3D m-SC [6].

Above all, structure control is still the most important factor in exploring the property limits of different kinds of electrode materials. Although excellent efforts have been made on developing carbon film electrode with better volumetric and areal capacitances, the value is still lower than that of pseudocapacitive materials, which is limited by the theoretical limits of EDLC. For the pseudocapacitive materials such as molybdenum oxide, it is possible to optimize the intrinsic electrochemical property by structure design, i.e., to obtain both good rate capability and cyclability as well as keep relatively high capacitance. However, the application of the oxides is seriously limited by the electrolyte condition, which is always a disadvantage compared with carbon materials. Pseudocapacitive carbon materials represent another promising trend to achieve balanced performance. In-plane m-SCs with interdigital architectures have proven its success to fabricate fast response devices with carbon electrodes. Thus, further study on the interplay effect between such architecture and pseudocapacitive materials is in need. Exploring 3D architecture for m-SC is a difficult but attracting challenge.

## Acknowledgements

The authors are grateful to the financial support by the National Basic Research Program of China (973 program, Grant No. 2013CB934301), the National Natural Science Foundation of China (Grant No. 51531006 and No. 51572148), the Research Project of Chinese Ministry of Education (Grant No. 113007A), and the Tsinghua University Initiative Scientific Research Program.

## Author details

Can Liu<sup>1</sup> and Zhengjun Zhang<sup>2\*</sup>

\*Address all correspondence to: zjzhang@tsinghua.edu.cn

1 Institute for Catalysis, Hokkaido University, Sapporo, Japan

2 School of Materials Science and Engineering, Key Laboratory of Advanced Materials, Tsinghua University, Beijing, People's Republic of China

## References

- [1] K.B. Lee, L.W. Lin, Electrolyte-based on-demand and disposable microbattery, *J Microelectromech S*, 2003;12:840–847. doi:10.1109/Jmems.2003.820272
- [2] A.H. Epstein, S.D. Senturia, G. Anathasuresh, A. Ayon, K. Breuer, K.S. Chen, F. Ehrich, G. Gauba, R. Ghodssi, C. Groshenry, S. Jacobson, J. Lang, C.C. Mehra, J.M. Miranda, S. Nagle, D. Orr, E. Piekos, M. Schmidt, G. Shirley, S. Spearing, C. Tan, Y.S. Tzeng, I. Waitz, Power MEMS and microengines, in: 1997 International Conference on Solid State Sensors and Actuators, 1997. TRANSDUCERS '97 Chicago, vol. 2, 1997, pp. 753–756 vol. 752.
- [3] A.H. Epstein, S.D. Senturia, Macro power from micro machinery, *Science*, 1997;276:1211–1211. doi:10.1126/science.276.5316.1211
- [4] A. Mehra, Z. Xin, A.A. Ayon, I.A. Waitz, M.A. Schmidt, C.M. Spadaccini, A six-wafer combustion system for a silicon micro gas turbine engine, *J Microelectromech S*, 2000;9:517–527. doi:10.1109/84.896774
- [5] J.W. Long, B. Dunn, D.R. Rolison, H.S. White, Three-dimensional battery architectures, *Chem Rev*, 2004;104:4463–4492. doi:10.1021/cr020740l
- [6] M. Beidaghi, Y. Gogotsi, Capacitive energy storage in micro-scale devices: recent advances in design and fabrication of micro-supercapacitors, *Energy Environ Sci*, 2014;7:867–884. doi:10.1039/C3EE43526A
- [7] Z.L. Wang, Self-powered nanosensors and nanosystems, *Adv Mater*, 2012;24:280–285. doi:10.1002/adma.201102958
- [8] J.-H. Sung, S.-J. Kim, S.-H. Jeong, E.-H. Kim, K.-H. Lee, Flexible micro-supercapacitors, *J Power Sources*, 2006;162:1467–1470. doi:10.1016/j.jpowsour.2006.07.043
- [9] I. Hyun Jin, S. Kumar, S.-H. Yang, G. Barbastathis, Origami fabrication of nanostructured, three-dimensional devices: electrochemical capacitors with carbon electrodes, *Appl Phys Lett*, 2006;88:083104. doi:10.1063/1.2177639
- [10] Y.Q. Jiang, Q. Zhou, L. Lin, Planar MEMS supercapacitor using carbon nanotube forests, in: 2009 IEEE 22nd International Conference on Micro Electro Mechanical Systems. MEMS 2009, 2009, pp. 587–590. doi:10.1109/memsys.2009.4805450
- [11] D. Pech, M. Brunet, P.-L. Taberna, P. Simon, N. Fabre, F. Mesnilgrete, V. Conedera, H. Durou, Elaboration of a microstructured inkjet-printed carbon electrochemical capacitor, *J Power Sources*, 2010;195:1266–1269. doi:10.1016/j.jpowsour.2009.08.085
- [12] J. Chmiola, C. Largeot, P.-L. Taberna, P. Simon, Y. Gogotsi, Monolithic carbide-derived carbon films for micro-supercapacitors, *Science*, 2010;328:480–483. doi:10.1126/science.1184126

- [13] D. Pech, M. Brunet, H. Durou, P. Huang, V. Mochalin, Y. Gogotsi, P.-L. Taberna, P. Simon, Ultrahigh-power micrometre-sized supercapacitors based on onion-like carbon, *Nat Nanotechnol*, 2010;5:651–654. doi:10.1038/nnano.2010.162
- [14] J. Feng, X. Sun, C. Wu, L. Peng, C. Lin, S. Hu, J. Yang, Y. Xie, Metallic few-layered VS<sub>2</sub> ultrathin nanosheets: high two-dimensional conductivity for in-plane supercapacitors, *J Am Chem Soc*, 2011;133:17832–17838. doi:10.1021/ja207176c
- [15] W. Gao, N. Singh, L. Song, Z. Liu, A.L.M. Reddy, L. Ci, R. Vajtai, Q. Zhang, B. Wei, P.M. Ajayan, Direct laser writing of micro-supercapacitors on hydrated graphite oxide films, *Nat Nanotechnol*, 2011;6:496–500. doi:10.1038/nnano.2011.110
- [16] K. Wang, W. Zou, B. Quan, A. Yu, H. Wu, P. Jiang, Z. Wei, An all-solid-state flexible micro-supercapacitor on a chip, *Adv Energy Mater*, 2011;1:1068–1072. doi:10.1002/aenm.201100488
- [17] M.F. El-Kady, R.B. Kaner, Scalable fabrication of high-power graphene micro-supercapacitors for flexible and on-chip energy storage, *Nat Commun*, 2013;4:1475–1475. doi:10.1038/ncomms2446
- [18] S. Makino, Y. Yamauchi, W. Sugimoto, Synthesis of electro-deposited ordered mesoporous RuO<sub>x</sub> using lyotropic liquid crystal and application toward micro-supercapacitors, *J Power Sources*, 2013;227:153–160. doi:10.1016/j.jpowsour.2012.11.032
- [19] M. Beidaghi, Y. Gogotsi, Capacitive energy storage in micro-scale devices: recent advances in design and fabrication of micro-supercapacitors, *Energy Environ Sci*, 2014;7:867–884. doi:10.1039/C3EE43526A
- [20] E.N. Hoffman, G. Yushin, T. El-Raghy, Y. Gogotsi, M.W. Barsoum, Micro and mesoporosity of carbon derived from ternary and binary metal carbides, *Microporous Mesoporous Mater*, 2008;112:526–532. doi:10.1016/j.micromeso.2007.10.033
- [21] M. Heon, S. Lofland, J. Applegate, R. Nolte, E. Cortes, J.D. Hettinger, P.-L. Taberna, P. Simon, P. Huang, M. Brunet, Y. Gogotsi, Continuous carbide-derived carbon films with high volumetric capacitance, *Energy Environ Sci*, 2011;4:135–138. doi:10.1039/c0ee00404a
- [22] P. Huang, M. Heon, D. Pech, M. Brunet, P.-L. Taberna, Y. Gogotsi, S. Lofland, J.D. Hettinger, P. Simon, Micro-supercapacitors from carbide derived carbon (CDC) films on silicon chips, *J Power Sources*, 2013;225:240–244. doi:10.1016/j.jpowsour.2012.10.020
- [23] C. Shen, X. Wang, W. Zhang, F. Kang, A high-performance three-dimensional micro supercapacitor based on self-supporting composite materials, *J Power Sources*, 2011;196:10465–10471. doi:10.1016/j.jpowsour.2011.08.007
- [24] F. Liu, A. Gutes, C. Carraro, J. Chu, R. Maboudian, Graphitization of n-type polycrystalline silicon carbide and its application for micro-supercapacitors, in: 2011 16th International Solid-State Sensors, Actuators and Microsystems Conference, 2011, pp. 1879–1882.

- [25] L. Wei, N. Nitta, G. Yushin, Lithographically patterned thin activated carbon films as a new technology platform for on-chip devices, *ACS Nano*, 2013;7:6498–6506. doi: 10.1021/nl4028129
- [26] X. Yang, C. Cheng, Y. Wang, L. Qiu, D. Li, Liquid-mediated dense integration of graphene materials for compact capacitive energy storage, *Science*, 2013;341:534–537.
- [27] T. Lin, I.W. Chen, F. Liu, C. Yang, H. Bi, F. Xu, F. Huang, Nitrogen-doped mesoporous carbon of extraordinary capacitance for electrochemical energy storage, *Science*, 2015;350:1508–1513. doi:10.1126/science.aab3798
- [28] X. Cui, R. Lv, R.U.R. Sagar, C. Liu, Z. Zhang, Reduced graphene oxide/carbon nanotube hybrid film as high performance negative electrode for supercapacitor, *Electrochimica Acta*, 2015;169:342–350. doi:10.1016/j.electacta.2015.04.074
- [29] D. Pech, M. Brunet, H. Durou, P. Huang, V. Mochalin, Y. Gogotsi, P.-L. Taberna, P. Simon, Ultrahigh-power micrometre-sized supercapacitors based on onion-like carbon, *Nat Nano*, 2010;5:651–654. <http://www.nature.com/nnano/journal/v5/n9/abs/nnano.2010.162.html#supplementary-information>
- [30] J.J. Yoo, K. Balakrishnan, J. Huang, V. Meunier, B.G. Sumpter, A. Srivastava, M. Conway, A.L.M. Reddy, J. Yu, R. Vajtai, P.M. Ajayan, Ultrathin planar graphene supercapacitors, *Nano Lett.*, 2011;11:1423–1427. doi:10.1021/nl200225j
- [31] M. Kaempgen, C.K. Chan, J. Ma, Y. Cui, G. Gruner, Printable thin film supercapacitors using single-walled carbon nanotubes, *Nano Lett.*, 2009;9:1872–1876. doi:10.1021/nl8038579
- [32] C. Portet, G. Yushin, Y. Gogotsi, Electrochemical performance of carbon onions, nanodiamonds, carbon black and multiwalled nanotubes in electrical double layer capacitors, *Carbon*, 2007;45:2511–2518. doi:10.1016/j.carbon.2007.08.024
- [33] M. Beidaghi, C. Wang, Micro-supercapacitors based on interdigital electrodes of reduced graphene oxide and carbon nanotube composites with ultrahigh power handling performance, *Adv Funct Mater*, 2012;22:4501–4510. doi:10.1002/adfm.201201292
- [34] Z.S. Wu, K. Parvez, X. Feng, K. Müllen, Graphene-based in-plane micro-supercapacitors with high power and energy densities, *Nat Commun*, 2013;4. doi:10.1038/ncomms3487
- [35] J.H. Lim, D.J. Choi, H.K. Kim, W.I. Cho, Y.S. Yoon, Thin film supercapacitors using a sputtered RuO<sub>2</sub> electrode, *J Electrochem Soc*, 2001;148:A275–A278. doi: 10.1149/1.1350666
- [36] C.-C. Liu, D.-S. Tsai, D. Susanti, W.-C. Yeh, Y.-S. Huang, F.-J. Liu, Planar ultracapacitors of miniature interdigital electrode loaded with hydrous RuO<sub>2</sub> and RuO<sub>2</sub> nanorods, *Electrochim Acta*, 2010;55:5768–5774. doi:10.1016/j.electacta.2010.05.015

- [37] J.P. Zheng, T.R. Jow, Q.X. Jia, X.D. Wu, Proton insertion into ruthenium oxide film prepared by pulsed laser deposition, *J Electrochem Soc*, 1996;143:1068–1070. doi: 10.1149/1.1836584
- [38] B.E. Conway, Transition from “Supercapacitor” to “Battery” behavior in electrochemical energy storage, *J Electrochem Soc*, 1991;138:1539–1548. doi:10.1149/1.2085829
- [39] T.M. Dinh, A. Achour, S. Vizireanu, G. Dinescu, L. Nistor, K. Armstrong, D. Guay, D. Pech, Hydrrous RuO<sub>2</sub>/carbon nanowalls hierarchical structures for all-solid-state ultrahigh-energy-density micro-supercapacitors, *Nano Energy*, 2014;10:288–294. doi: 10.1016/j.nanoen.2014.10.003
- [40] C. Shen, X. Wang, W. Zhang, F. Kang, Direct prototyping of patterned nanoporous carbon: a route from materials to on-chip devices, *SciRep*, 2013;3:2294. doi:10.1038/srep02294
- [41] J.H. Pikul, H. Gang Zhang, J. Cho, P.V. Braun, W.P. King, High-power lithium ion microbatteries from interdigitated three-dimensional bicontinuous nanoporous electrodes, *Nat Commun*, 2013;4:1732. doi:10.1038/ncomms2747
- [42] H.-S. Min, B.Y. Park, L. Taherabadi, C. Wang, Y. Yeh, R. Zaouk, M.J. Madou, B. Dunn, Fabrication and properties of a carbon/polypyrrole three-dimensional microbattery, *J Power Sources*, 2008;178:795–800. doi: 10.1016/j.jpowsour.2007.10.003
- [43] M. Kotobuki, Y. Suzuki, H. Munakata, K. Kanamura, Y. Sato, K. Yamamoto, T. Yoshida, Effect of sol composition on solid electrode/solid electrolyte interface for all-solid-state lithium ion battery, *Electrochimica Acta*, 2011;56:1023–1029. doi:10.1016/j.electacta.2010.11.008
- [44] C. Shen, X. Wang, S. Li, J.g. Wang, W. Zhang, F. Kang, A high-energy-density micro supercapacitor of asymmetric MnO<sub>2</sub>-carbon configuration by using micro-fabrication technologies, *J Power Sources*, 2013;234:302–309. doi:10.1016/j.jpowsour.2012.10.101
- [45] W. Zhou, X. Cao, Z. Zeng, W. Shi, Y. Zhu, Q. Yan, H. Liu, J. Wang, H. Zhang, One-step synthesis of Ni<sub>3</sub>S<sub>2</sub> nanorod@Ni(OH)(2) nanosheet core-shell nanostructures on a three-dimensional graphene network for high-performance supercapacitors, *Energy Environ Sci*, 2013;6:2216–2221. doi:10.1039/c3ee40155c
- [46] H.Y. Lee, J.B. Goodenough, Supercapacitor behavior with KCl electrolyte, *J Solid State Chem*, 1999;144:220–223. doi:10.1006/jssc.1998.8128
- [47] P. Simon, Y. Gogotsi, Materials for electrochemical capacitors, *Nat Mater*, 2008;7:845–854.
- [48] S.C. Pang, M.A. Anderson, T.W. Chapman, Novel electrode materials for thin-film ultracapacitors: comparison of electrochemical properties of sol-gel-derived and electrodeposited manganese dioxide, *J Electrochem Soc*, 2000;147:444–450. doi: 10.1149/1.1393216

- [49] C.-C. Lin, P.-Y. Lin, Capacitive manganese oxide thin films deposited by reactive direct current sputtering, *J Electrochem Soc*, 2010;157:A753–A759. doi:10.1149/1.3414823
- [50] D.F. Yang, Pulsed laser deposition of manganese oxide thin films for supercapacitor applications, *J Power Sources*, 2011;196:8843–8849. doi:10.1016/j.jpowsour.2011.06.045
- [51] I. Zhitomirsky, J. Wei, N. Nagarajan, Manganese oxide films for electrochemical supercapacitors, *J Mater Process Technol*, 2007;186:356–361. doi:10.1016/j.jmatprotec.2007.01.003
- [52] W. Si, C. Yan, Y. Chen, S. Oswald, L. Han, O.G. Schmidt, On chip, all solid-state and flexible micro-supercapacitors with high performance based on MnOx/Au multilayers, *Energy Environ Sci*, 2013;6:3218–3223. doi:10.1039/C3EE41286E
- [53] M. Nakayama, A. Tanaka, Y. Sato, T. Tonosaki, K. Ogura, Electrodeposition of manganese and molybdenum mixed oxide thin films and their charge storage properties, *Langmuir*, 2005;21:5907–5913. doi:10.1021/la050114u
- [54] M. Nakayama, K. Suzuki, K. Okamura, R. Inoue, L. Athouel, O. Crosnier, T. Brousse, Doping of cobalt into multilayered manganese oxide for improved pseudocapacitive properties, *J Electrochem Soc*, 2010;157:A1067–A1072. doi:10.1149/1.3467865
- [55] D.F. Yang, Pulsed laser deposition of vanadium-doped manganese oxide thin films for supercapacitor applications, *J Power Sources*, 2013;228:89–96. doi:10.1016/j.jpowsour.2012.11.067
- [56] S.K. Meher, G.R. Rao, Effect of microwave on the nanowire morphology, optical, magnetic, and pseudocapacitance behavior of Co<sub>3</sub>O<sub>4</sub>, *J Phys Chem C*, 2011;115:25543–25556. doi:10.1021/jp209165v
- [57] L. Gu, Y. Wang, R. Lu, W. Wang, X. Peng, J. Sha, Silicon carbide nanowires@Ni(OH)<sub>2</sub> core-shell structures on carbon fabric for supercapacitor electrodes with excellent rate capability, *J Power Sources*, 2015;273:479–485. doi:10.1016/j.jpowsour.2014.09.113
- [58] G.Q. Zhang, H.B. Wu, H.E. Hoster, M.B. Chan-Park, X.W. Lou, Single-crystalline NiCo<sub>2</sub>O<sub>4</sub> nanoneedle arrays grown on conductive substrates as binder-free electrodes for high-performance supercapacitors, *Energy Environ Sci*, 2012;5:9453–9456. doi:10.1039/C2EE22572G
- [59] C. Liu, Z. Li, Z. Zhang, MoOx thin films deposited by magnetron sputtering as an anode for aqueous micro-supercapacitors, *Sci Technol Adv Mater*, 2013;14. 065005. doi: 10.1088/1468-6996/14/6/065005
- [60] C. Liu, Z. Li, Z. Zhang, Molybdenum oxide film with stable pseudocapacitive property for aqueous micro-scale electrochemical capacitor, *Electrochimica Acta*, 2014;134:84–91. doi: 10.1016/j.electacta.2014.04.115

- [61] E. Eustache, R. Frappier, R.L. Porto, S. Bouhtiyya, J.-F. Pierson, T. Brousse, Asymmetric electrochemical capacitor microdevice designed with vanadium nitride and nickel oxide thin film electrodes, *Electrochem Commun*, 2013;28:104–106.
- [62] C. Liu, Z. Xie, W. Wang, Z. Li, Z. Zhang, Fabrication of MoO<sub>x</sub> film as a conductive anode material for micro-supercapacitors by electrodeposition and annealing, *J Electrochem Soc*, 2014;161:A1051–A1057. doi:10.1149/2.081406jes
- [63] C. Liu, Z. Xie, W. Wang, Z. Li, Z. Zhang, The Ti@MoO<sub>x</sub> nanorod array as a three dimensional film electrode for micro-supercapacitors, *Electrochem Commun*, 2014;44:23–26. doi:10.1016/j.elecom.2014.04.007
- [64] V. Presser, L. Zhang, J.J. Niu, J. McDonough, C. Perez, H. Fong, Y. Gogotsi, Flexible nano-felts of carbide-derived carbon with ultra-high power handling capability, *Adv Energy Mater*, 2011;1:423–430. doi:10.1002/aenm.201100047
- [65] Z. Niu, L. Zhang, L. Liu, B. Zhu, H. Dong, X. Chen, All-solid-state flexible ultrathin micro-supercapacitors based on graphene, *Adv Mater (Deerfield Beach, Fla.)*, 2013;25:4035–4042. doi:10.1002/adma.201301332
- [66] B. Hsia, M.S. Kim, M. Vincent, C. Carraro, R. Maboudian, Photoresist-derived porous carbon for on-chip micro-supercapacitors, *Carbon*, 2013;57:395–400. doi:10.1016/j.carbon.2013.01.089
- [67] S.W. Lee, B.-S. Kim, S. Chen, Y. Shao-Horn, P.T. Hammond, Layer-by-layer assembly of all carbon nanotube ultrathin films for electrochemical applications, *J Am Chem Soc*, 2009;131:671–679. doi:10.1021/ja807059k
- [68] C. Arbizzani, M. Mastragostino, L. Meneghello, Polymer-based redox supercapacitors: a comparative study, *Electrochimica Acta*, 1996;41:21–26. doi:10.1016/0013-4686(95)00289-Q
- [69] J.C. Carlberg, O. Inganäs, Poly(3,4-ethylenedioxythiophene) as electrode material in electrochemical capacitors, *J Electrochem Soc*, 1997;144:L61–L64. doi:10.1149/1.1837553
- [70] W. Sun, R. Zheng, X. Chen, Symmetric redox supercapacitor based on micro-fabrication with three-dimensional polypyrrole electrodes, *J Power Sources*, 2010;195:7120–7125. doi:10.1016/j.jpowsour.2010.05.012
- [71] M. Beidaghi, C. Wang, Micro-supercapacitors based on three dimensional interdigital polypyrrole/C-MEMS electrodes, *Electrochimica Acta*, 2011;56:9508–9514. doi:10.1016/j.electacta.2011.08.054
- [72] D.R. Rolison, J.W. Long, J.C. Lytle, A.E. Fischer, C.P. Rhodes, T.M. McEvoy, M.E. Bourg, A.M. Lubers, Multifunctional 3D nanoarchitectures for energy storage and conversion, *Chem Soc Rev*, 2009;38:226–252. doi:10.1039/b801151f



